

Bounds to precision for an SU(1,1) interferometer with Gaussian input states

Qian-Kun Gong¹, Dong Li¹, Chun-Hua Yuan^{1,4}, * Z. Y. Ou^{1,3}, and Weiping Zhang^{2,4}

¹Quantum Institute for Light and Atoms, Department of Physics,
East China Normal University, Shanghai 200062, P. R. China

² Department of Physics and Astronomy, Shanghai Jiao Tong University, Shanghai 200240, P. R. China

³Department of Physics, Indiana University-Purdue University Indianapolis,
402 North Blackford Street, Indianapolis, Indiana 46202, USA and

⁴Collaborative Innovation Center of Extreme Optics,
Shanxi University, Taiyuan, Shanxi 030006, P. R. China

(Dated: October 30, 2018)

We theoretically present the quantum Cramér-Rao bounds (QCRB) of an SU(1,1) interferometer for Gaussian states input with and without the internal photonic losses. The phase shifts in the single arm and in the double arms are studied and the corresponding analytical expressions of quantum Fisher information with Gaussian input states are presented. Different from the traditional Mach-Zehnder interferometer, the QCRB of single arm case is slightly higher or lower than that of double arms case depending on the input states. With a fixed mean photon number and for pure Gaussian state input, the optimal sensitivity is achieved with a squeezed vacuum input in one mode and the vacuum input in the other. We compare the QCRB with the standard quantum limit and Heisenberg limit. In the case of small internal losses the QCRB can beat the standard quantum limit.

PACS numbers: 42.50.St, 03.65.Ta, 03.67.-a, 42.50.Dv

I. INTRODUCTION

Quantum enhanced metrology which has received a lot of attention in recent years is the use of quantum measurement techniques to obtain higher statistical precision than purely classical approaches [1–13]. Mach-Zehnder interferometer (MZI) and its variants have been used as a generic model to realize precise estimation of phase. In order to achieve the ultimate lower bounds [14, 15], much work has been devoted to find the methods to improve the sensitivity of phase estimation. Overall, three main lines of research have been pursued. (1) Using the non-classical input states. Caves [3] suggested to replace the unused port with the squeezed-vacuum light to reach a sub-shot-noise sensitivity. Xiao *et al.* [16] and Grangier *et al.* [17] have demonstrated the experimental results beyond the standard quantum limit (SQL). Using the NOON states of the form $(|N\rangle_a|0\rangle_b + e^{i\phi_N}|0\rangle_a|N\rangle_b)/\sqrt{2}$, the phase-sensing measurements can reach the Heisenberg limit (HL) [18, 19]. (2) Using new detection methods, such as the homodyne detection [20] and the parity detection [21–24], etc. (3) Amplitude [25] or phase [13] magnification using nonlinear process. Here we focus on the nonlinear beam splitters to amplify the amplitude. In 1986, Yurke *et al.* [25] introduced a new type of interferometer where two nonlinear beam splitters take the place of two linear beam splitters (BSs) in the traditional MZI. It is also called the SU(1,1) interferometer because it is described by the SU(1,1) group, as opposed to the traditional SU(2) MZI for beam splitters (BSs). The detailed quantum statistics of the two-mode SU(1,1) interferome-

ter was studied by Leonhardt [26]. SU(1,1) phase states also have been studied theoretically in quantum measurements for phase-shift estimation [27, 28]. Plick *et al.* [29] proposed to inject a strong coherent beam to “boost” the photon number. Experimental realization of this SU(1,1) optical interferometer was reported by different groups [30, 31]. The noise performance of this interferometer was analyzed [11, 32] and under the same phase-sensing intensity condition the improvement of 4.1 dB in signal-to-noise ratio was observed [33]. By contrast, an SU(1,1) atomic interferometer also has been experimentally realized with Bose-Einstein Condensates [34–38]. In addition, an SU(1,1)-typed atom-light hybrid interferometer [39] is reported, where the atomic Raman amplification processes is used as the nonlinear beam splitters. The atom-light correlations have also been used to enhance the sensitivity of atom interferometer [40–43]. Furthermore, this SU(1,1)-type hybrid correlated interferometer was also proposed in the circuit quantum electrodynamics system [44], which provides a different method for basic measurement using the hybrid interferometers.

Quantum parameter estimation theory establishes the ultimate lower bound to the sensitivity with which a classical parameter (e.g., phase shift ϕ) that parameterizes the quantum state can be measured. In general, it is difficult to optimize over the input state that is fed into the interferometer to obtain the optimal estimation protocols. One of the popular ways to obtain the lower bounds in quantum metrology, is to use the method of the quantum Fisher information (QFI) [4, 5]. The so-called QFI is defined by maximizing the Fisher information over all possible measurement strategies allowed by quantum mechanics. It characterizes the maximum amount of information that can be extracted from quantum experiments about an unknown parameter using the best (and ideal) measurement device. It establishes the best precision

*Electronic address: chyuan@phy.ecnu.edu.cn

that can be attained with a given quantum probe. In recent years, to obtain the QFI many efforts have been made by theory [53–65] and experiments [66, 67].

Since interferometers as a generic model to realize precise estimation of phase shift, the corresponding QFI has been studied. For the MZI, Jarzyna *et al.* [57] studied the QFIs between phase shifts in the single arm case and in the two-arm case and presented the differences between them. For SU(1,1) interferometer, some QFI results of phase shift only in one arm [58, 65] and in the two arms [36] have been studied. However, the effect of losses on QFI in an SU(1,1) interferometer has not been investigated yet. In this paper, we study QFI in an SU(1,1) interferometer without and with losses with the phase shifts in the two arms and give the differences of corresponding QCRBs between the phase shifts in the single arm and two arms. We also compare the QCRB with the SQL and Heisenberg limit (HL) where the lossy QCRB can still beat the SQL with small internal loss.

Our article is organized as follows. In Sec. II, we briefly review the SU(1,1) interferometer and the QFI. In Sec. III, we give the QFIs in an ideal SU(1,1) interferometer with the phase shifts in double arms, and compare the corresponding QCRBs to ones with the phase shift in single arm. In Sec. IV, the QFIs in a lossy SU(1,1) interferometer with phase shifts in single arm and in double arm are given, as well the QCRBs. Finally, we conclude with a summary of our results.

II. SU(1,1) INTERFEROMETER AND QCRB

The traditional Mach-Zehnder interferometer is called an SU(2) interferometer, where the transformation through the interferometer is a rotation on angular momentum observables

$$\begin{aligned}\hat{J}_x &= \frac{\hbar}{2}(\hat{a}^\dagger \hat{b} + \hat{a} \hat{b}^\dagger), \hat{J}_y = -\frac{i\hbar}{2}(\hat{a}^\dagger \hat{b} - \hat{a} \hat{b}^\dagger), \\ \hat{J}_z &= \frac{\hbar}{2}(\hat{a}^\dagger \hat{a} - \hat{b}^\dagger \hat{b}).\end{aligned}\quad (1)$$

where \hat{a} (\hat{a}^\dagger) and \hat{b} (\hat{b}^\dagger) are the annihilation (creation) operators for the two modes, respectively. By contrast, an SU(1,1) interferometer is shown in Fig. 1(a), where the nonlinear beams splitters (NBSs) (such as, optical parametrical amplifier (OPA) or four-wave mixing) replaced the 50-50 beam splitters in a traditional MZI. We first give a brief review of the SU(1,1) interferometer introduced by Yurke *et al.* [25] and the QCRB. For the SU(1,1) interferometer, the induced transformation on the input observables is that of the group SU(1,1). To describe the SU(1,1) interferometer, the Hermitian operators are introduced [25], which are given by

$$\begin{aligned}\hat{K}_x &= \frac{\hbar}{2}(\hat{a}^\dagger \hat{b}^\dagger + \hat{a} \hat{b}), \hat{K}_y = -\frac{i\hbar}{2}(\hat{a}^\dagger \hat{b}^\dagger - \hat{a} \hat{b}), \\ \hat{K}_z &= \frac{\hbar}{2}(\hat{a}^\dagger \hat{a} + \hat{b}^\dagger \hat{b} + 1).\end{aligned}\quad (2)$$

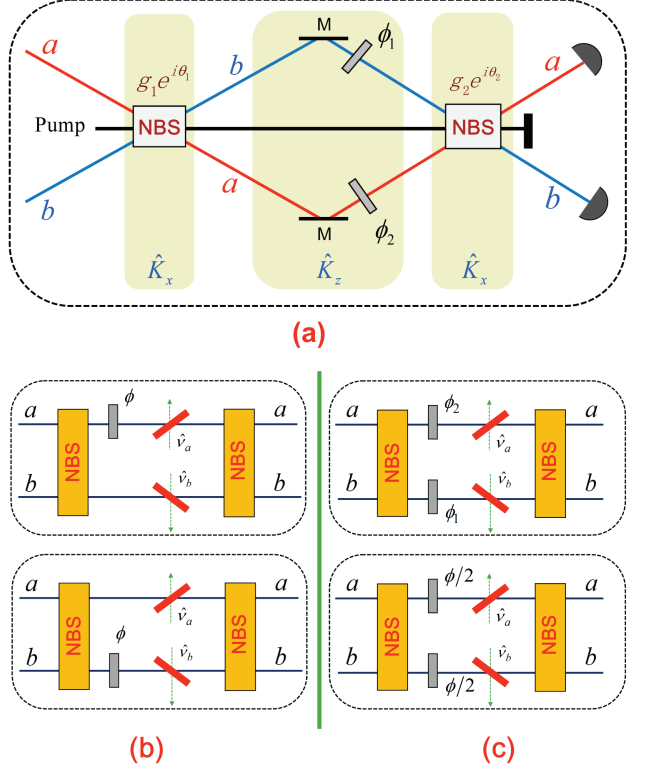


FIG. 1: (Color online) (a) The schematic diagram of the SU(1,1) interferometer. Two nonlinear beam splitters (NBSs) take the place of two beam splitters in the traditional Mach-Zehnder interferometer, and \hat{J}_i ($i = x, y, z$) replaced by \hat{K}_i ($i = x, y, z$) in Schwinger representation. g_1 (g_2) and θ_1 (θ_2) describe the strength and phase shift in the NBS process 1 (2), respectively. a and b ($i = 0, 1, 2$) denote two light modes in the interferometer. ϕ_1 , ϕ_2 : phase shifts; M : mirrors; BS : beam splitter. (b) and (c) A lossy SU(1,1) interferometer model. The losses inside the interferometer are modeled by adding the fictitious beam splitters. \hat{v}_a and \hat{v}_b are the vacuum. (b) Phase shift in the single arm is divided into single upper arm and single lower arm due to the intensities of the two arms are not equal. (c) Phase shifts in the double arms. Phase shifts in the double arms for the SU(1,1) interferometer, $\phi/2$ in the down arm is instead of $-\phi/2$ for MZI due to the difference between \hat{J}_z and \hat{K}_z .

The initial state $|\psi_{in}\rangle$ injecting into a NBS results in the output $|\Psi\rangle = e^{-i\xi\hat{K}_x}|\psi_{in}\rangle$ where ξ is squeezed parameter [68]. After the first NBS, the two beams sustain phase shifts, i.e., \hat{a} undergoes a phase shift of ϕ_2 and \hat{b} undergoes a phase shift of ϕ_1 . In the Schrödinger picture the state vector is transformed as $|\Psi_\phi\rangle = e^{-i\phi\hat{K}_z}|\Psi\rangle$, where $\phi = -(\phi_1 + \phi_2)$ [69].

To obtain the sensitivity of phase-shift measurements with various input states, the Fisher information (FI) F is determined by the measurement statistics used to estimate the value of ϕ . If a positive operator-valued measure (POVM) $\{\hat{\Pi}_i\}$ describes a measurement on the modified probe state $|\Psi_\phi\rangle$, then the FI F is given by

[4, 5, 53–55]

$$F = \sum_i \frac{1}{\langle \Psi_\phi | \hat{\Pi}_i | \Psi_\phi \rangle} \left(\frac{\partial \langle \Psi_\phi | \hat{\Pi}_i | \Psi_\phi \rangle}{\partial \phi} \right)^2. \quad (3)$$

Various observables may lead to different FIs F . However, the QFI \mathcal{F} is at least as great as the FI F for the optimal observable and gives upper bound of F . The QFI \mathcal{F} is the intrinsic information in the quantum state and is not related to actual measurement procedure. In terms of the complete basis $\{|k\rangle\}$ such that $\hat{\rho}(\phi) = \sum_k p_k |k\rangle \langle k|$ with $p_k \geq 0$ and $\sum_k p_k = 1$, the QFI can be written as [4, 5, 53–55]

$$\mathcal{F} = \sum_{k,k'} \frac{2}{p_k + p_{k'}} |\langle k | \partial_\phi \hat{\rho}(\phi) | k' \rangle|^2. \quad (4)$$

Whatever the measurement chosen, the QCRB can give the lower bound for the phase measurement [4, 5, 53–55]

$$\Delta\phi_{\mathcal{F}} = \frac{1}{\sqrt{\mathcal{F}}}. \quad (5)$$

III. QCRB IN AN IDEAL SU(1,1) INTERFEROMETER

In general, the QFI bounds depend on the way that the interferometer phase delay is modeled: (I) phase shift only in the single arm, (II) phase shift distributed symmetrically, which is shown in Fig. 1(b) and (c). Hereafter, we use the single arm case (S) and double-arm case (D) to denote them. For the MZI, the QFIs between the single arm case and double arm case have been studied by Jarzyna *et al.* [57]. The phase shifts in single upper arm and in single lower arm are the same. For the coherent light combined with a squeezed vacuum light input ($|\psi_{in}\rangle = |\alpha\rangle_a \otimes |0, \varsigma\rangle_b$, where $\alpha = |\alpha| e^{i\theta_\alpha}$, $N_\alpha = |\alpha|^2$ and $|0, \varsigma\rangle_b = \hat{S}_b(r)|0\rangle_b$ is the single-mode squeezed vacuum state in the b -mode, and $\hat{S}_b(r) = \exp[(\varsigma^* \hat{b}^2 - \varsigma \hat{b}^{\dagger 2})/2]$ with $\varsigma = r \exp(i\theta_\varsigma)$ is the squeezing parameter), the relation of QFIs is given by

$$\mathcal{F}_{\text{MZI,coh\&squ}}^S = \frac{\sinh^2(2r)}{2} + N_\alpha + \mathcal{F}_{\text{MZI,coh\&squ}}^D, \quad (6)$$

where $\mathcal{F}_{\text{MZI,coh\&squ}}^D = N_\alpha e^{2r} + \sinh^2 r$, and the superscripts S and D denote the single arm case and double arm case, respectively. In the ideal SU(1,1) interferometer, the QFIs in the two cases are also different. Sparaciari *et al.* [58] have studied some QFI results in the one arm case of the SU(1,1) interferometer. Next, we give the QFIs with various input states in the case of phase shifts on two arms.

Under the condition of lossless, the QFI for a pure state is given by [57]

$$\mathcal{F} = 4(\langle \Psi'_\phi | \Psi'_\phi \rangle - |\langle \Psi'_\phi | \Psi_\phi \rangle|^2), \quad (7)$$

where $|\Psi_\phi\rangle$ is the state vector just before the second NBS of the SU(1,1) interferometer and $|\Psi'_\phi\rangle = \partial|\Psi_\phi\rangle/\partial\phi$. For the state $|\Psi\rangle (= e^{-i\xi\hat{K}_x} |\psi_{in}\rangle)$ inside the interferometer, $|\Psi'_\phi\rangle = -i\hat{K}_z e^{-i\phi\hat{K}_z} |\Psi\rangle$, and the QFI is

$$\mathcal{F} = 4\Delta^2 \hat{K}_z, \quad (8)$$

where $\Delta^2 \hat{K}_z = \langle \Psi | \hat{K}_z^2 | \Psi \rangle - \langle \Psi | \hat{K}_z | \Psi \rangle^2$. For two-mode interferometers, the QFI \mathcal{F} can be written as

$$\mathcal{F} = \Delta^2 \hat{n}_a + \Delta^2 \hat{n}_b + 2\text{Cov}[\hat{n}_a, \hat{n}_b], \quad (9)$$

where $\hat{n}_a = \hat{a}^\dagger \hat{a}$, $\hat{n}_b = \hat{b}^\dagger \hat{b}$, $\Delta^2 \hat{n}_j = \langle \Psi | \hat{n}_j^2 | \Psi \rangle - \langle \Psi | \hat{n}_j | \Psi \rangle^2$ ($j = a, b$) and $\text{Cov}[\hat{n}_a, \hat{n}_b] = \langle \Psi | \hat{n}_a \hat{n}_b | \Psi \rangle - \langle \Psi | \hat{n}_a | \Psi \rangle \langle \Psi | \hat{n}_b | \Psi \rangle$. The QFI \mathcal{F} is composed of the photon number fluctuations in each arm and the correlation between two arms.

The transformation through the first NBS inside an SU(1,1) interferometer is given by $\hat{a}_{out} = u\hat{a}_{in} + v\hat{b}_{in}^\dagger$, $\hat{b}_{out} = u\hat{b}_{in} + v\hat{a}_{in}^\dagger$, where $u = \cosh g$, $v = \sinh g e^{i\theta_g}$, and $g (= \xi/2)$ describes the strength of the NBS [70]. For two coherent states $|\alpha\rangle \otimes |\beta\rangle$ ($j = |j| e^{i\theta_j}$, $N_j = |j|^2$, $j = \alpha, \beta$) input case, we have

$$\begin{aligned} \mathcal{F}_{\text{coh\&coh}}^D &= (N_\alpha + N_\beta) \cosh(4g) + \sinh^2(2g) \\ &+ 2 \sinh(4g) \sqrt{N_\alpha N_\beta} \cos(\theta_\alpha + \theta_\beta - \theta_g). \end{aligned} \quad (10)$$

When $\theta_\alpha + \theta_\beta - \theta_g = 0$, we obtain the maximal QFI $\mathcal{F}_{\text{coh\&coh}}^D = (N_\alpha + N_\beta) \cosh(4g) + \sinh^2(2g) + 2 \sinh(4g) \sqrt{N_\alpha N_\beta}$. When $N_\alpha = N_\beta = 0$ (vacuum input) and $N_\alpha \neq 0$, $N_\beta = 0$ (one coherent state input), from Eq. (10) the corresponding QFIs are given by

$$\mathcal{F}_{\text{vac}}^D = \sinh^2(2g), \quad (11)$$

and

$$\mathcal{F}_{\text{coh\&vac}}^D = N_\alpha \cosh 4g + \sinh^2(2g). \quad (12)$$

Next, we consider a coherent light combined with a squeezed vacuum light as the input, and the QFI is given by

$$\begin{aligned} \mathcal{F}_{\text{coh\&squ}}^D &= \cosh^2(2g) \left[\frac{1}{2} \sinh^2(2r) + N_\alpha \right] + \sinh^2(2g) \\ &\times [N_\alpha (\cosh 2r - \sinh 2r \cos \Phi) + \cosh^2 r], \end{aligned} \quad (13)$$

where $\Phi = \theta_\varsigma + 2\theta_\alpha - 2\theta_g$. When $\Phi = \pi$, we can obtain the maximal QFI $\mathcal{F}_{\text{coh\&squ}}^D = \cosh^2(2g) [\sinh^2(2r)/2 + N_\alpha] + \sinh^2(2g) [N_\alpha e^{2r} + \cosh^2 r]$. When $r = 0$, $\mathcal{F}_{\text{coh\&squ}}^D$ also reduces to $\mathcal{F}_{\text{coh\&vac}}^D$, which matches the above result. This input state has been used to improve the phase-shift measurement sensitivity in the SU(1,1) interferometer but only by the method of the error propagation in Ref. [20].

So far, we have given the QFI of the SU(1,1) interferometer where the phase shifts in the two arms as shown in Fig. 1. The QFIs of different phase shifts are summarized in the Table I. Sparaciari *et al.* [58] have studied

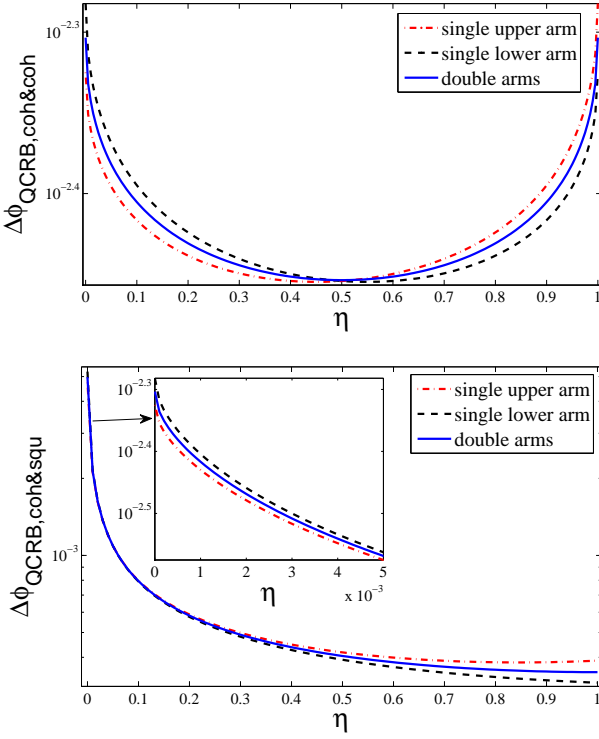


FIG. 2: (Color online) The QCRB versus the η for two coherent states input (upper) and coherent \otimes squeezed state input (lower). The inset in lower figure shows a zoom of the graph for small values of η . Parameters: $N_{\text{in}} = 200$, and $g = 1.5$.

some QFI results of phase shift in upper arm for the SU(1,1) interferometer. But the intensities in two arms of the interferometer are asymmetry unless the input intensity of two arms are equal. Then the QFIs of phase shift in upper arm and in lower arm are slightly different, and we complement the single arm case of phase shift in lower arm. The differences of optimal phase sensitivities $\Delta\phi_{\text{QCRB}}$ from single arm case and double arm case depend on the input states of two mode. For vacuum state input and one coherent state input, two input states have certain relations as well as the phase sensitivities, which is obtained from the Table I. For one coherent state input, the QCRB of single arm case is slightly higher or lower than that of double arm case due to the term $N_\alpha(1 \pm 2 \cosh 2g)$. To describe the effect on the QCRB from the unbalanced input state, we introduce a parameter η which is defined by

$$\eta = \frac{\text{mean photon number of } b \text{ mode}}{\text{total mean photon number of input}}. \quad (14)$$

For the two coherent states input and coherent \otimes squeezed vacuum state input, η is equal to N_β/N_{in} ($N_{\text{in}} = N_\alpha + N_\beta$) and $\sinh^2 r/N_{\text{in}}$ ($N_{\text{in}} = N_\alpha + \sinh^2 r$), respectively. The optimal phase sensitivities $\Delta\phi_{\text{QCRB}}$ as a function of η are shown in Fig. 2. When η is small, the $\Delta\phi_{\text{QCRB}}$ from the single upper arm case is the best. But when η is large, the $\Delta\phi_{\text{QCRB}}$ from the single lower arms case is the best.

Therefore, for Gaussian states input, the $\Delta\phi_{\text{QCRB}}$ from the double arm case is always an intermediate value.

Next, we compare the optimal phase sensitivities $\Delta\phi_{\text{QCRB}}$ between single arm case and double arm case with the SQL and HL, which are given by

$$\Delta\phi_{\text{SQL}} = \frac{1}{\sqrt{\bar{n}}}, \quad \Delta\phi_{\text{HL}} = \frac{1}{\bar{n}}. \quad (15)$$

Here \bar{n} is the total mean photon number inside the SU(1,1) interferometer not the total input photon number as that in the traditional MZI. Because the MZI is linear, the phase-sensing photon number is equal to input number. But the phase-sensing photon number inside the SU(1,1) interferometer is amplified compared to the input number. The mean photon number \bar{n} in the SU(1,1) interferometer is given by

$$\bar{n} \equiv \langle \Psi | \hat{n}_a + \hat{n}_b | \Psi \rangle. \quad (16)$$

For different input states, the mean photon number \bar{n} inside the SU(1,1) interferometer are respectively given by

$$\begin{aligned} \bar{n}_{\text{vac}} &= 2 \sinh^2 g, \quad \bar{n}_{\text{coh\&vac}} = \cosh(2g) N_{\text{in}}^{\text{coh\&vac}} + 2 \sinh^2 g, \\ \bar{n}_{\text{coh\&coh}} &= \cosh(2g) N_{\text{in}}^{\text{coh\&coh}} + 2 \sinh^2 g \\ &\quad + 2 \sqrt{N_\alpha N_\beta} \sinh 2g \cos(\theta_\alpha + \theta_\beta - \theta_g), \\ \bar{n}_{\text{coh\&squ}} &= \cosh(2g) N_{\text{in}}^{\text{coh\&squ}} + 2 \sinh^2 g, \end{aligned} \quad (17)$$

where N_{in}^j ($j = \text{coh\&vac}, \text{coh\&coh}$ and coh\&squ) is the total average photon number of different input, and their average photon numbers $N_{\text{in}}^{\text{coh\&vac}}$, $N_{\text{in}}^{\text{coh\&coh}}$, and $N_{\text{in}}^{\text{coh\&squ}}$ are N_α , $N_\alpha + N_\beta$, and $N_\alpha + \sinh^2 r$, respectively.

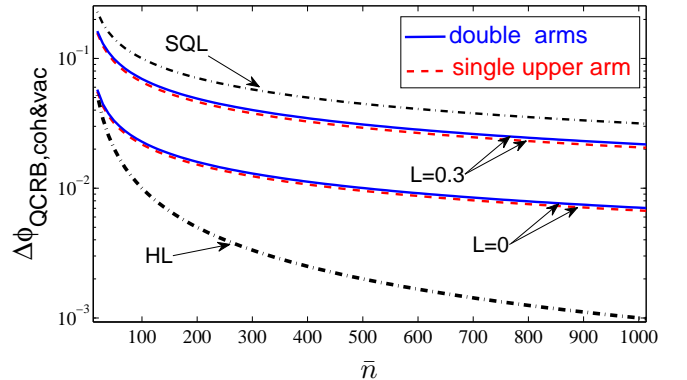


FIG. 3: (Color online) The QCRB as a function of the mean photon number \bar{n} inside the SU(1,1) interferometer for coherent state input with different loss rates. The thin and thick dashed-dotted lines are SQL and HL, respectively. Parameter: $g = 1.5$.

For vacuum state input, the corresponding QCRB from Eq. (5) is $\Delta\phi_{\text{QCRB, vac}} = 1/\sqrt{\mathcal{F}_{\text{vac}}^{\text{D}}} = 1/\sinh(2g) = 1/\sqrt{\bar{n}_{\text{vac}}(2 + \bar{n}_{\text{vac}})}$ is the same as result of Yurke *et al.* [25]. The ideal QCRBs as a function of the mean photon

number \bar{n} inside the SU(1,1) interferometer are plotted by the dashed lines in Figs. 3-4. The sensitivity $\Delta\phi_{\mathcal{F}}$ improve with increasing \bar{n} , and they can beat SQL. For one coherent state input and phase shift in the single upper arm, the QCRB of single upper arm is slightly higher than that of double arm case due to $N_{\alpha}(1+2\cosh 2g) > 0$ as shown in Fig. 3. In Fig. 4, the QCRB of double arm case is slightly higher than that of single upper arm case because we select a specific parameters ($N_b \gg N_a$) makes the term $N_{\alpha} + N_{\beta} + 2(N_{\alpha} - N_{\beta})\cosh 2g < 0$. For coherent \otimes squeezed vacuum state input and fixed g and r , $(\Delta\phi^S - \Delta\phi^D)_{QCRB,coh\&squ}$ is greater than zero at the beginning and soon less than 0 with the increase of \bar{n} (N_{α}) as shown in Fig. 5.

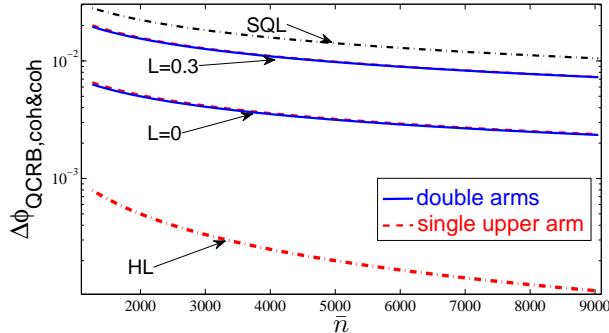


FIG. 4: (Color online) The QCRB as a function of the mean photon number \bar{n} inside the SU(1,1) interferometer for two coherent states input with different loss rates. The thin and thick dashed-dotted lines are SQL and HL, respectively. Parameter: $g = 1.5$ and $N_b = 3N_a$.

IV. QCRB IN A LOSSY SU(1,1) INTERFEROMETER

In the presence of realistic imperfections and noise, the ultimate precision limit in noisy quantum-enhanced metrology was also studied [45–52]. But as far as we know, the QFI of lossy SU(1,1) interferometer is still missing. In this section, we investigate the effects of losses on the QCRB in an SU(1,1) interferometer. As shown in Fig. 1(b) and (c), losses can be modeled by adding the fictitious beam splitters [71]. \hat{v}_a and \hat{v}_b are the vacuum, and T_i are the transmission parameters where $T_i = 1 - L_i$ with the losses rate L_i ($i = 1, 2$). For convenience, we consider both arms of the interferometer to have the same internal loss rates L . For photons loss before or after the phase shift, the QCRBs of them are the same after the numerical comparison, which agrees with the results from the method of Kraus operators [71].

Recently, Gao *et al.* [62] developed a formula to analyze the QCRB with Gaussian states which is related to mean values and covariance matrix of annihilation (creation) operators of the corresponding modes. In the

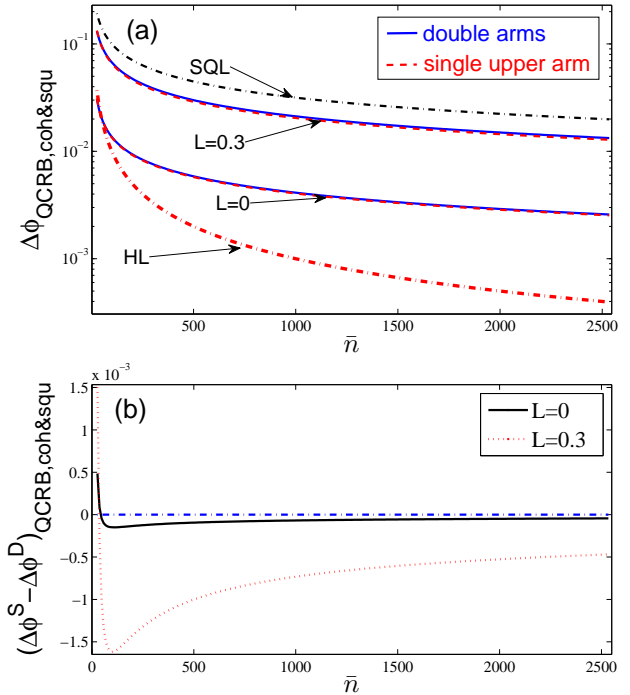


FIG. 5: (Color online) (a) The QCRB as a function of the mean photon number \bar{n} inside the SU(1,1) interferometer for coherent state and vacuum squeezed state input with different loss rates. The thin and thick dashed-dotted lines are SQL and HL, respectively. (b) $(\Delta\phi^S - \Delta\phi^D)_{QCRB,coh\&squ}$ versus the mean photon number \bar{n} for $L = 0$ and $L = 0.3$. Parameters: $g = 1.5$ and $r = 1.5$.

SU(1,1) interferometer, if input states are Gaussian, the outputs are also Gaussian. This is due to Gaussian operation of OPAs and BSs. We use this model to obtain the QFI in the presence of losses. For single arm case, we only consider the phase shift in the upper arm because they have similar behaviors for phase shift in the upper or lower arm. According to Ref. [62], the QFI is given by

$$\mathcal{F}^{\text{loss}} = \frac{1}{2} \text{Tr} \left\{ \partial_{\phi} \Sigma [\Sigma (\partial_{\phi} \Sigma)^{-1} \Sigma^T + \frac{1}{4} \Omega (\partial_{\phi} \Sigma)^{-1} \Omega^T]^{-1} \right\} + (\partial_{\phi} \bar{\mathbf{d}})^T (\Sigma)^{-1} (\partial_{\phi} \bar{\mathbf{d}}), \quad (18)$$

where $\partial_{\phi} \Sigma = \partial \Sigma / \partial \phi$ and $\partial_{\phi} \bar{\mathbf{d}} = \partial \bar{\mathbf{d}} / \partial \phi$. The definitions of matrix Ω , the column vector of expectation values $\bar{\mathbf{d}}$ and its covariance matrix Σ are described in Ref. [72].

A. The QRCB of coherent \otimes squeezed states input

For coherent and squeezed states are injected, according to Eq. (13), we set $\theta_{\alpha} = \theta_g = 0$, $\theta_{\zeta} = \pi$ and the QFIs with losses for single arm case and double arm case are

respectively worked out as

$$\mathcal{F}_{\text{coh\&squ}}^{\text{loss, S}} = \frac{N_{\text{coh\&squ}}^{\text{loss, S}}}{D_{\text{coh\&squ}}^{\text{loss, S}}}, \quad (19)$$

$$\begin{aligned} \mathcal{F}_{\text{coh\&squ}}^{\text{loss, D}} &= \frac{(1-L)[1+e^{2r}\tanh^2(2g)]+e^{2r}L/\cosh(2g)}{L[e^{2r}L/(1-L)+(e^{2r}+1)\cosh(2g)-1]+1} \\ &\times N_\alpha \cosh^2(2g) + \frac{C^{\text{D}}}{D^{\text{D}}}, \end{aligned} \quad (20)$$

where $N_{\text{coh\&squ}}^{\text{loss, S}}$, $D_{\text{coh\&squ}}^{\text{loss, S}}$, C^{D} and D^{D} are very complex and their derivation processes are given in supplemental materials. For $N_\alpha = 0$, $r = 0$ and $N_\alpha \neq 0$, $r = 0$, the QFIs $\mathcal{F}_{\text{coh\&squ}}^{\text{loss, } j}$ ($j = \text{S, D}$) reduce to the results with loss for only vacuum state input and only one coherent state input, respectively.

Then for coherent and squeezed vacuum state input, the corresponding quantum Cramér-Rao bound from Eq. (5) is given by

$$\Delta\phi_{\text{QCRB, coh\&squ}}^{\text{loss, } j} = \frac{1}{\sqrt{\mathcal{F}_{\text{coh\&squ}}^{\text{loss, } j}}} \quad (j = \text{S, D}). \quad (21)$$

When $L = 0$, the QRCB $\Delta\phi_{\text{QCRB, coh\&squ}}^{\text{loss, } j}$ ($j = \text{S, D}$) can reduce to the ideal lossless results $\Delta\phi_{\text{QCRB, coh\&squ}}^j = 1/\sqrt{\mathcal{F}_{\text{coh\&squ}}^j}$, where the maximal $\mathcal{F}_{\text{coh\&squ}}^j$ are given in the Table I.

If vacuum input ($N_\alpha = 0$ and $r = 0$), combined with Eqs. (19)-(21), the QCRBs with loss for two different cases are the same and worked out as

$$\Delta\phi_{\text{QCRB, vac}}^{\text{loss}} = \frac{1}{\sqrt{\mathcal{F}_{\text{vac}}^{\text{loss}}}}, \quad (22)$$

where $\mathcal{F}_{\text{vac}}^{\text{loss}} = (1-L)^2 \sinh^2(2g)/\{L[L+\cosh(2g)-1]+1\}$. Without losses ($L = 0$), Eq. (22) reduces to $\Delta\phi_{\text{QCRB, vac}}^{\text{loss}} = 1/\sinh(2g)$, which is the same as result of Yurke *et al.* without losses case [25]. With one coherent state input ($N_\alpha \neq 0$ and $r = 0$), the QCRB with losses from Eq. (21) is found to be

$$\Delta\phi_{\text{QCRB, coh\&vac}}^{\text{loss, } j} = \frac{1}{\sqrt{\mathcal{F}_{\text{coh\&vac}}^{\text{loss, } j}}} \quad (j = \text{S, D}). \quad (23)$$

For phase shift in single upper arm case, we have

$$\mathcal{F}_{\text{coh\&vac}}^{\text{loss, S}} = X^{\text{S}}/Y^{\text{S}}, \quad (24)$$

where

$$\begin{aligned} X^{\text{S}} &= 2(1-L)\cosh^2 g\{(1-L)[(N_\alpha+1)L(1-L) \\ &\times \cosh(4g)+(2N_\alpha(2L^2-L+1)+(2L-1)^2) \\ &\times \cosh(2g)]+N_\alpha L(3L^2-4L+3) \\ &+ (1-L)(-3L^2+3L-1)\}, \end{aligned} \quad (25)$$

$$Y^{\text{S}} = [2(1-L)L\sinh^2 g+1][4(1-L)L\sinh^2 g+1], \quad (26)$$

and for phase shift in double arm case, we have

$$\mathcal{F}_{\text{coh\&vac}}^{\text{loss, D}} = X^{\text{D}}/Y^{\text{D}}, \quad (27)$$

where

$$\begin{aligned} X^{\text{D}} &= (1-L)\{(1-L)^2 \cosh(6g)(N_\alpha+1)L+(1-L) \\ &\times \cosh(4g)[(3L^2-2L+2)N_\alpha+2L(L-1)+1] \\ &+ L\cosh(2g)[N_\alpha(3L^2-4L+3)-(1-L)^2] \\ &+ (1-L)(L^2N_\alpha-2L^2+2L-1)\}, \\ Y^{\text{D}} &= 2Y^{\text{S}}. \end{aligned} \quad (28)$$

B. The QRCB of two coherent states input

For two coherent states ($|\alpha\rangle \otimes |\beta\rangle$) input, for convenience we let $\theta_g = \theta_\alpha = 0$, then the QFIs with loss for phase shift in the single upper arm is worked out as

$$\mathcal{F}_{\text{coh\&coh}}^{\text{loss, S}} = \frac{N_{\text{coh\&coh}}^{\text{loss, S}}}{D_{\text{coh\&coh}}^{\text{loss, S}}}, \quad (29)$$

where

$$\begin{aligned} N_{\text{coh\&coh}}^{\text{loss, S}} &= (1-L)\{(1-L)\sinh^2(2g)[4(1-L)L\sinh^2 g \\ &+ 1]+4[(1-L)\cosh(2g)+L][2(1-L)L\sinh^2 g+1] \\ &\times [N_\alpha \cosh^2 g+N_\beta \sinh^2 g+\sqrt{N_\alpha N_\beta} \sinh(2g) \cos \theta_\beta]\}, \\ D_{\text{coh\&coh}}^{\text{loss, S}} &= Y^{\text{S}}, \end{aligned} \quad (30)$$

and for phase shift in the double arm is worked out as

$$\mathcal{F}_{\text{coh\&coh}}^{\text{loss, D}} = \frac{N_{\text{coh\&coh}}^{\text{loss, D}}}{D_{\text{coh\&coh}}^{\text{loss, D}}}, \quad (31)$$

where

$$\begin{aligned} N_{\text{coh\&coh}}^{\text{loss, D}} &= L(1-L)\cosh(2g)[(N_\alpha+N_\beta)(3L^2-4L+3) \\ &- (1-L)^2]+(1-L)^2 \cosh(4g)[(N_\alpha+N_\beta)(3L^2-2L \\ &+ 2)+(2L^2-2L+1)]+L(1-L)^3 \cosh(6g)(N_\alpha+N_\beta \\ &+ 1)+(1-L)^2[(N_\alpha+N_\beta)L^2-(2L^2-2L+1)] \\ &+ 4\sqrt{N_\alpha N_\beta}(1-L)\sinh(2g)\cos(\theta_\beta)[(1-L)(3L^2-2L \\ &+ 2)\cosh(2g)+L((1-L)^2 \cosh 4g+2L^2-3L+2)], \\ D_{\text{coh\&coh}}^{\text{loss, D}} &= Y^{\text{D}}. \end{aligned} \quad (32)$$

$\mathcal{F}_{\text{coh\&coh}}^{\text{loss, } j}$ ($j = \text{S, D}$) are complex and their derivation process are given in the supplemental materials. The difference of QFIs of two different phase shifts is given by

$$\begin{aligned} &\mathcal{F}_{\text{coh\&coh}}^{\text{loss, S}} - \mathcal{F}_{\text{coh\&coh}}^{\text{loss, D}} \\ &= \frac{1-L}{4(1-L)L\sinh^2 g-1} \times \{\cosh(2g)[N_a(2-L) \\ &+ N_b(3L-2)]+N_b(1-3L)+N_a(1+L) \\ &+ 2\sqrt{N_a N_b} L \sinh(2g) \cos(\theta_\beta)\}. \end{aligned} \quad (33)$$

When $L = 0$, $\mathcal{F}_{\text{coh\&coh}}^{\text{loss, S}} - \mathcal{F}_{\text{coh\&coh}}^{\text{loss, D}} = N_\alpha + N_\beta + 2(N_\alpha - N_\beta) \cosh 2g$, which agrees with the ideal difference of $\mathcal{F}_{\text{coh\&coh}}^{\text{S}} - \mathcal{F}_{\text{coh\&coh}}^{\text{D}}$ from other method. When $g = 0$, $\mathcal{F}_{\text{coh\&coh}}^{\text{loss, S}} - \mathcal{F}_{\text{coh\&coh}}^{\text{loss, D}} = (1 - L)(3N_a - N_b)$.

With two coherent states input, the QCRB with losses from Eqs. (29) and (31) is found to be

$$\Delta\phi_{\text{QCRB,coh\&coh}}^{\text{loss, } j} = \frac{1}{\sqrt{\mathcal{F}_{\text{coh\&coh}}^{\text{loss, } j}}} \quad (j = \text{S, D}). \quad (34)$$

Without losses ($L = 0$), Eq. (34) is simplified to $\Delta\phi_{\text{QCRB,coh\&coh}}^j = 1/\sqrt{\mathcal{F}_{\text{coh\&coh}}^j}$ ($j = \text{S, D}$), where the maximal $\mathcal{F}_{\text{coh\&coh}}^j$ are given in the Table I.

Figures 3-5 show the QCRB as a function of the mean photon number \bar{n} inside the SU(1,1) interferometer. In the presence of small losses ($L = 0.3$), the QCRB can beat the SQL for both single arm and double arm cases. When the loss inside the interferometer continues to increase, the QCRB is unable to reach below the SQL. For the coherent \otimes squeezed vacuum state input and given g and r , as shown in Fig. 5, the difference of $\mathcal{F}_{\text{coh\&squ}}^{\text{loss, S}} - \mathcal{F}_{\text{coh\&squ}}^{\text{loss, D}}$ is from positive to negative due to the increase of N_α .

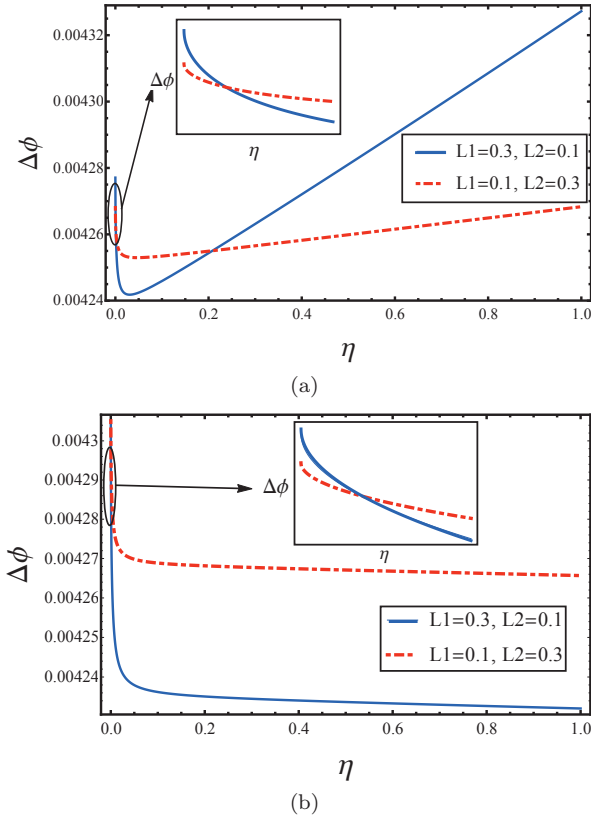


FIG. 6: (Color online) The QCRB as a function of the squeezing fraction of the mean photon number η with different loss rates L_1 and L_2 (a) for single arm case and (b) double arms case. The inset shows a zoom of the graph for small values of η . Parameters: $N_{\text{in}} = 200$, and $g = 1.5$.

V. DISCUSSION AND CONCLUSION

Because the coherent \otimes squeezed vacuum state ($|\alpha\rangle_a \otimes |0, \zeta\rangle_b$) input, the QCRB can approach the HL under a certain condition. Then we further analyze the QCRB of state for different parameters. The parameter $\eta = \sinh^2 r/N_{\text{in}}$ ($N_{\text{in}} = N_\alpha + \sinh^2 r$) can be used to label the squeezing fraction of the mean photon number. When $\eta = 0$ or $\eta = 1$, the input state is only a coherent state $|\alpha\rangle_a$ or a squeezed vacuum state $|0, \zeta\rangle_b$. When $0 < \eta < 1$, the input state is a coherent \otimes squeezed vacuum state. For single upper arm case and a given fixed N_{in} , as shown in Fig. 6(a), there is an optimal value η to obtain the highest QCRB due to losses, which is different from ideal case as shown in Fig. 2 (lower). But for double arm case, as shown in Fig. 6(b), the optimal value η is 1. That is for a given fixed N_{in} , only the squeezed vacuum light as input and without the coherent state, the phase sensitivity is the highest, which is the same as that of ideal case in Fig. 2 (lower).

Now we analyze the effect on the QCRB of different loss rates L_1 (upper arm) and L_2 (lower arm) in two channels and compare the QCRBs of their exchanges in two arms. As shown in Fig. 6(a), for single upper arm case and the phase shift in a (upper) channel, the QCRB is higher when the loss of the upper arm is greater than that of the lower arm. As shown in Fig. 6(b), the above conclusion for double arm case is also right. Because the loss in the arm input by the squeezed vacuum state is greater influence on the precision of QCRB.

In conclusion, we have presented the analytical expressions of QFI of an SU(1,1) interferometer for Gaussian state input under the ideal and lossy conditions. The phase shift in the single arm and in the double arm are compared. For single arm case, the QCRB of phase shift in upper arm and in lower arm are different slightly due to the intensities in two interferometric arms are not symmetry. We also compare the QCRBs between the phase shift in one arm and the phase shifts in double arm. For coherent state \otimes squeezed state input and with a definite input number of photons, the optimal conditions to obtain the highest phase sensitivity of different phase shift ways are different. In the presence of small internal loss, the lossy QCRB can beat the SQL. For a fixed mean photon number and with pure Gaussian input, the optimal sensitivity is obtained with a squeezed vacuum in one mode and the vacuum in the other.

Acknowledgements

This work was supported by the National Basic Research Program of China (973 Program) under Grant No. 2011CB921604 and the National Natural Science Foundation of China under Grant Nos. 11474095, 11234003, and 11129402 and the Fundamental Research Funds for the Central Universities.

[1] C. W. Helstrom, *Quantum Detection and Estimation Theory* (Academic, New York, 1976).

[2] A. S. Holevo, *Probabilistic and Statistical Aspect of Quantum Theory* (North-Holland, Amsterdam, 1982).

[3] C. M. Caves, Quantum-mechanical noise in an interferometer, *Phys. Rev. D* **23**, 1693 (1981).

[4] S. L. Braunstein and C. M. Caves, Statistical Distance and the Geometry of Quantum States, *Phys. Rev. Lett.* **72**, 3439 (1994).

[5] S. L. Braunstein, C. M. Caves, and G. J. Milburn, Generalized Uncertainty Relations: Theory, Examples, and Lorentz Invariance, *Ann. Phys.* **247** 135 (1996).

[6] H. Lee, P. Kok, and J. P. Dowling, A Quantum Rosetta Stone for Interferometry, *J. Mod. Opt.* **49** 2325 (2002).

[7] V. Giovannetti, S. Lloyd, and L. Maccone, Quantum Metrology, *Phys. Rev. Lett.* **96**, 010401 (2006).

[8] M. Zwierz, C. A. Pérez-Delgado, and P. Kok, General Optimality of the Heisenberg Limit for Quantum Metrology, *Phys. Rev. Lett.* **105**, 180402 (2010).

[9] V. Giovannetti, S. Lloyd, and L. Maccone, Quantum-enhanced measurements: beating the standard quantum limit, *Science* **306**, 1330 (2004);

[10] V. Giovannetti, S. Lloyd, and L. Maccone, Advances in quantum metrology, *Nature photonics* **5**, 222 (2011).

[11] Z. Y. Ou, Enhancement of the phase-measurement sensitivity beyond the standard quantum limit by a nonlinear interferometer, *Phys. Rev. A* **85**, 023815 (2012).

[12] B. P. Abbott *et al.* (LIGO Scientific Collaboration and Virgo Collaboration), Observation of Gravitational Waves from a Binary Black Hole Merger, *Phys. Rev. Lett.* **116**, 061102 (2016).

[13] O. Hosten, R. Krishnakumar, N. J. Engelsen, M. A. Kasevich, Quantum phase magnification, *Science* **352**, 1552 (2016).

[14] M. Zwierz, C. A. Pérez-Delgado, and P. Kok, Ultimate limits to quantum metrology and the meaning of the Heisenberg limit, *Phys. Rev. A* **85**, 042112 (2012).

[15] L. Pezzè, P. Hyllus, and A. Smerzi, Phase-sensitivity bounds for two-mode interferometers, *Phys. Rev. A* **91**, 032103 (2015).

[16] M. Xiao, L. A. Wu, and H. J. Kimble, Precision Measurement beyond the Short Noise Limit, *Phys. Rev. Lett.* **59**, 278 (1987).

[17] P. Grangier, R. E. Slusher, B. Yurke, and A. LaPorta, Squeezed-Light-Enhanced Polarization Interferometer, *Phys. Rev. Lett.* **59**, 2153 (1987).

[18] J. P. Dowling, Quantum optical metrology—the low-down on high-N00N states, *Contemporary Physics* **49**, 125 (2008).

[19] A. N. Boto, P. Kok, D. S. Abrams, S. L. Braunstein, C. P. Williams, and J. P. Dowling, Quantum Interferometric Optical Lithography: Exploiting Entanglement to Beat the Diffraction Limit, *Phys. Rev. Lett.* **85**, 2733 (2000).

[20] D. Li, C. H. Yuan, Z. Y. Ou, and W. P. Zhang, The phase sensitivity of an SU(1,1) interferometer with coherent and squeezed-vacuum light, *New J. Phys.* **16**, 073020 (2014).

[21] P. M. Anisimov, G. M. Raterman, A. Chiruvelli, W. N. Plick, S. D. Huver, H. Lee, and J. P. Dowling, Quantum Metrology with Two-Mode Squeezed Vacuum: Parity Detection Beats the Heisenberg Limit, *Phys. Rev. Lett.* **104**, 103602 (2010).

[22] C. C. Gerry and J. Mimih, The parity operator in quantum optical metrology, *Contemporary Physics* **51**, 497 (2010).

[23] A. Chiruvelli and H. Lee, Parity measurements in quantum optical metrology, *Journal of Modern Opt.* **58**, 945 (2011).

[24] D. Li, Bryan T. Gard, Y. Gao, C.-H. Yuan, W. Zhang, H. Lee, J. P. Dowling, Phase sensitivity at the Heisenberg limit in an SU(1,1) interferometer via parity detection, *arXiv:1603.09019*

[25] B. Yurke, S. L. McCall, and J. R. Klauder, SU(2) and SU(1,1) interferometers, *Phys. Rev. A* **33**, 4033 (1986).

[26] U. Leonhardt, Quantum statistics of a two-mode SU(1,1) interferometer, *Phys. Rev. A* **49**, 1231 (1994).

[27] A. Vourdas, SU(2) and SU(1,1) phase states, *Phys. Rev. A* **41**, 1653 (1990).

[28] B. C. Sanders, G. J. Milburn and Z. Zhang, Optimal quantum measurements for phase-shift estimation in optical interferometry, *J. Mod. Opt.* **44**, 1309 (1997).

[29] W. N. Plick, J. P. Dowling, and G. S. Agarwal, Coherent-light-boosted sub-shot noise quantum interferometry, *New J. Phys.* **12**, 083014 (2010).

[30] J. Jing, C. Liu, Z. Zhou, Z. Y. Ou, and W. Zhang, Realization of a Nonlinear Interferometer with Parametric Amplifiers, *Appl. Phys. Lett.* **99**, 011110 (2011).

[31] T. S. Horrom, B. E. Anderson, P. Gupta, and P. Lett, SU(1,1) interferometry via four-wave mixing in Rb. The 45th Winter Colloquium on the Physics of Quantum Electronics (PQE), 2015.

[32] A. M. Marino, N. V. Corzo Trejo and P. D. Lett, Effect of losses on the performance of an SU(1,1) interferometer, *Phys. Rev. A* **86**, 023844 (2012).

[33] F. Hudelist, J. Kong, C. Liu, J. Jing, Z. Y. Ou, and W. Zhang, Quantum metrology with parametric amplifier based photon correlation interferometers, *Nat. Commun.* **5**, 3049 (2014).

[34] C. Gross, T. Zibold, E. Nicklas, J. Estève, and M. K. Oberthaler, Nonlinear atom interferometer surpasses classical precision limit, *Nature (London)* **464**, 1165 (2010).

[35] Daniel Linnemann, Realization of an SU(1,1) Interferometer with Spinor Bose-Einstein Condensates, Master thesis, University of Heidelberg, 2013.

[36] D. Linnemann, H. Strobel, W. Muessel, J. Schulz, R. J. Lewis-Swan, K. V. Kheruntsyan, and M. K. Oberthaler, Quantum-Enhanced Sensing Based on Time Reversal of Nonlinear Dynamics, *Phys. Rev. Lett.* **117**, 013001 (2016).

[37] J. Peise, B. Lücke, L. Pezzè, F. Deuretzbacher, W. Ertmer, J. Arlt, A. Smerzi, L. Santos and C. Klemp, Interaction-free measurements by quantum Zeno stabilization of ultracold atoms, *Nat. Commun.* **6**, 6811 (2015).

[38] M. Gabrielli, L. Pezzè, and A. Smerzi, Spin-mixing interferometry with Bose-Einstein condensates, *Phys. Rev. Lett.* **115**, 163002 (2015).

[39] B. Chen, C. Qiu, S. Chen, J. Guo, L. Q. Chen, Z. Y. Ou, and W. Zhang, Atom-Light Hybrid Interferometer, *Phys. Rev. Lett.* **115**, 043602 (2015).

[40] J. Jacobson, G. Björk, and Y. Yamamoto, Quantum limit for the atom-light interferometer, *Appl. Phys. B* **60**, 187-191 (1995).

[41] S. A. Haine, Information-Recycling Beam Splitters for Quantum Enhanced Atom Interferometry, *Phys. Rev.*

Lett. **112**, 120405 (2014).

[42] S. S. Szigeti, B. Tonekaboni, W. Y. S. Lau, S. N. Hood, and S. A. Haine, Squeezed-light-enhanced atom interferometry below the standard quantum limit, Phys. Rev. A **90**, 063630 (2014).

[43] S. A. Haine, and W. Y. S. Lau, Generation of atom-light entanglement in an optical cavity for quantum enhanced atom interferometry, Phys. Rev. A **93**, 023607 (2016).

[44] Sh. Barzanjeh, D. P. DiVincenzo, and B. M. Terhal, Dispersive qubit measurement by interferometry with parametric amplifiers, Phys. Rev. B **90**, 134515 (2014).

[45] R. Demkowicz-Dobrzanski, U. Dorner, B. J. Smith, J. S. Lundeen, W. Wasilewski, K. Banaszek, and I. A. Walmsley, Quantum phase estimation with lossy interferometers, Phys. Rev. A **80**, 013825 (2009).

[46] B. M. Escher, R. L. de Matos Filho and L. Davidovich, General framework for estimating the ultimate precision limit in noisy quantum-enhanced metrology, Nat. Phys. **7**, 406 (2011).

[47] R. Demkowicz-Dobrzanski, J. Kolodynski, and M. Guta, The elusive Heisenberg limit in quantum-enhanced metrology, Nat. Commun. **3**, 1063 (2012).

[48] D. W. Berry, Michael J. W. Hall, and Howard M. Wiseman, Stochastic Heisenberg Limit: Optimal Estimation of a Fluctuating Phase, Phys. Rev. Lett. **111**, 113601 (2013).

[49] R. Chaves, J. B. Brask, M. Markiewicz, J. Kolodynski, and A. Acin, Noisy Metrology beyond the Standard Quantum Limit, Phys. Rev. Lett. **111**, 120401 (2013).

[50] W. Dur, M. Skotiniotis, F. Frowis, and B. Kraus, Improved Quantum Metrology Using Quantum Error Correction, Phys. Rev. Lett. **112**, 080801 (2014).

[51] E. M. Kessler, I. Lovchinsky, A. O. Sushkov, and M. D. Lukin, Quantum Error Correction for Metrology, Phys. Rev. Lett. **112**, 150802 (2014).

[52] S. Alipour, M. Mehboudi, and A. T. Rezakhani, Quantum Metrology in Open Systems: Dissipative Cramer-Rao Bound, Phys. Rev. Lett. **112**, 120405 (2014).

[53] G. Toth and I. Apellaniz, Quantum metrology from a quantum information science perspective, J. Phys. A **47**, 424006 (2014).

[54] L. Pezzè and A. Smerzi, in Proceedings of the International School of Physics “Enrico Fermi”, Course CLXXXVIII “Atom Interferometry” edited by G. Tino and M. Kasevich (Società Italiana di Fisica and IOS Press, Bologna, 2014), p. 691.

[55] R. Demkowicz-Dobrzanski, M. Jarzyna, J. Kolodynski, Quantum limits in optical interferometry, Progress in Optics **60**, 345 (2015).

[56] X.-B. Wang, T. Hiroshima, A. Tomita, M. Hayashi, Quantum information with Gaussian states, Opt. Reports **448**, 1 (2007).

[57] M. Jarzyna and R. Demkowicz-Dobrzanski, Quantum interferometry with and without an external phase reference, Phys. Rev. A **85**, 011801(R) (2012).

[58] C. Sparaciari, S. Olivares, and M. G. A. Paris, Gaussian-state interferometry with passive and active elements, Phys. Rev. A **93**, 023810 (2016).

[59] A. Monras, Phase space formalism for quantum estimation of Gaussian states, arXiv:1303.3682v1 (2013).

[60] O. Pinel, P. Jian, N. Treps, C. Fabre, and D. Braun, Quantum parameter estimation using general single-mode Gaussian states, Phys. Rev. A **88**, 040102(R) (2013).

[61] Jing Liu, Xiaoxing Jing, and Xiaoguang Wang, Phase-matching condition for enhancement of phase sensitivity in quantum metrology, Phys. Rev. A **88**, 042316 (2013).

[62] Y. Gao and H. Lee, Bounds on quantum multiple-parameter estimation with Gaussian state, Eur. Phys. J. D **68**, 347 (2014).

[63] Z. Jiang, Quantum Fisher information for states in exponential form, Phys. Rev. A **89**, 032128 (2014).

[64] D. Safranek, A. R. Lee, and I. Fuentes, Quantum parameter estimation using multi-mode Gaussian states, New J. Phys. **17**, 073016 (2015).

[65] C. Sparaciari, S. Olivares, and M. G. A. Paris, Bounds to precision for quantum interferometry with Gaussian states and operations, J. Opt. Soc. Am. B **32**, 1354 (2015).

[66] H. Strobel, W. Muessel, D. Linnemann, T. Zibold, D. B. Hume, L. Pezze, A. Smerzi, M. K. Oberthaler, Fisher information and entanglement of non-Gaussian spin states, Science **345**, 424 (2014).

[67] P. Hauke, M. Heyl, L. Tagliacozzo, and P. Zoller, Measuring multipartite entanglement through dynamic susceptibilities, Nat. Phys. **12**, 778 (2016).

[68] Two Hermitian operator \hat{K}_x and \hat{K}_y generate the two-mode squeezing operator $\hat{S}_{a_1 a_2}(\xi) = \exp(-\xi \hat{a}_1^\dagger \hat{a}_2^\dagger + \xi^* \hat{a}_1 \hat{a}_2) = \exp\left[-\frac{i}{\hbar}(2\xi_2 \hat{K}_x + 2\xi_1 \hat{K}_y)\right]$, where $\xi = \xi_1 + i\xi_2 = re^{i\theta}$ is the squeezed parameter of the nonlinear beam splitter.

[69] P. Kok and B. W. Lovett, Introduction to optical quantum information processing (Cambridge University Press, Cambridge, 2010), p. 515.

[70] H. Ma, D. Li, C.-H. Yuan, L. Q. Chen, Z. Y. Ou, and W. Zhang, SU(1,1)-type light-atom-correlated interferometer, Phys. Rev. A **92**, 023847 (2015).

[71] U. Dorner, R. Demkowicz-Dobrzanski, B. J. Smith, J. S. Lundeen, W. Wasilewski, K. Banaszek, and I. A. Walmsley, Optimal Quantum Phase Estimation, Phys. Rev. Lett. **102**, 040403 (2009).

[72] See Supplemental Material for details.

TABLE I: The maximal QFIs of the SU(1,1) interferometer for different phase delay ways with different input states.

input states	single arm \mathcal{F}^S		double arms \mathcal{F}^D
	phase shift in upper arm	phase shift in lower arm	
vacuum states	$\sinh^2(2g)$ [58]	$\sinh^2(2g)$	$\sinh^2(2g)$
one coherent state $ \alpha\rangle_a \otimes 0\rangle_b$	$N_\alpha \cosh 4g + \sinh^2(2g)$ $+N_\alpha(1 + 2 \cosh 2g)$ [58]	$N_\alpha \cosh 4g + \sinh^2(2g)$ $+N_\alpha(1 - 2 \cosh 2g)$	$N_\alpha \cosh 4g + \sinh^2(2g)$
two coherent state $ \alpha\rangle_a \otimes \beta\rangle_b$	$(N_\alpha + N_\beta) \cosh 4g + \sinh^2(2g)$ $+2\sqrt{N_\alpha N_\beta} \sinh 4g + N_\alpha + N_\beta$ $+2(N_\alpha - N_\beta) \cosh 2g$ [58]	$(N_\alpha + N_\beta) \cosh 4g + \sinh^2(2g)$ $+2\sqrt{N_\alpha N_\beta} \sinh 4g + N_\alpha + N_\beta$ $-2(N_\alpha - N_\beta) \cosh 2g$	$(N_\alpha + N_\beta) \cosh 4g + \sinh^2(2g)$ $+2\sqrt{N_\alpha N_\beta} \sinh 4g$
coherent \otimes squee -zed vacuum state $ \alpha\rangle_a \otimes \varsigma, 0\rangle_b$ $(\varsigma = r \exp(i\theta_\varsigma))$	$\cosh^2(2g)[\sinh^2(2r)/2 + N_\alpha]$ $+ \sinh^2(2g)[N_\alpha e^{2r} + \cosh^2 r]$ $+N_\alpha(1 + 2 \cosh 2g)$ $-\frac{1}{4}(\cosh 4r - 1)(2 \cosh 2g - 1)$	$\cosh^2(2g)[\sinh^2(2r)/2 + N_\alpha]$ $+ \sinh^2(2g)[N_\alpha e^{2r} + \cosh^2 r]$ $+N_\alpha(1 - 2 \cosh 2g)$ $+\frac{1}{4}(\cosh 4r - 1)(2 \cosh 2g + 1)$	$\cosh^2(2g)[\sinh^2(2r)/2 + N_\alpha]$ $+ \sinh^2(2g)[N_\alpha e^{2r} + \cosh^2 r]$

Supplemental Materials: Bounds to precision for an $SU(1,1)$ interferometer with Gaussian input states

Qian-Kun Gong¹, Dong Li¹, Chun-Hua Yuan^{1,4}, Z. Y. Ou^{1,3}, Weiping Zhang^{2,4}

¹Quantum Institute for Light and Atoms, Department of Physics, East China Normal University, Shanghai, 200241, P. R. China

²*Department of Physics and Astronomy, Shanghai Jiao Tong University, Shanghai 200240, P. R. China*

³*Department of Physics, Indiana University-Purdue University Indianapolis, 402 North Blackford Street, Indianapolis, Indiana 46202, USA*

⁴Collaborative Innovation Center of Extreme Optics, Shanxi University, Taiyuan, Shanxi 030006, P. R. China

The quantum Cramér-Rao bounds with loss

According to the formula in Ref. [1], we calculate the output of mean values and covariance matrix of quadrature operators through an SU(1,1) interferometer which is then followed by a transformation from quadrature operator basis to annihilation (creation) operator basis. \hat{a}_i (\hat{a}_i^\dagger), \hat{b}_i (\hat{b}_i^\dagger), \hat{v}_{ai} (\hat{v}_{ai}^\dagger) and \hat{v}_{bi} (\hat{v}_{bi}^\dagger) are the annihilation (creation) operators of a , b and two vacuum modes, respectively, as shown in Fig. 1. We introduce the quadrature operators

$$\begin{aligned}\hat{x}_{a_i} &= \hat{a}_i + \hat{a}_i^\dagger, \quad \hat{p}_{a_i} = -i(\hat{a}_i - \hat{a}_i^\dagger), \\ \hat{x}_{b_i} &= \hat{b}_i + \hat{b}_i^\dagger, \quad \hat{p}_{b_i} = -i(\hat{b}_i - \hat{b}_i^\dagger), \\ \hat{x}_{v_{ai}} &= \hat{v}_{ai} + \hat{v}_{ai}^\dagger, \quad \hat{p}_{v_{ai}} = -i(\hat{v}_{ai} - \hat{v}_{ai}^\dagger), \\ \hat{x}_{v_{bi}} &= \hat{v}_{bi} + \hat{v}_{bi}^\dagger, \quad \hat{p}_{v_{bi}} = -i(\hat{v}_{bi} - \hat{v}_{bi}^\dagger).\end{aligned}\tag{S1}$$

We define quadrature column vector

$$\begin{aligned} \mathbf{X}_i &= (\hat{X}_{i,1}, \hat{X}_{i,2}, \hat{X}_{i,3}, \hat{X}_{i,4}, \hat{X}_{i,5}, \hat{X}_{i,6}, \hat{X}_{i,7}, \hat{X}_{i,8})^\top \\ &\equiv (\hat{x}_{a_i}, \hat{p}_{a_i}, \hat{x}_{b_i}, \hat{p}_{b_i}, \hat{x}_{v_{ai}}, \hat{p}_{v_{ai}}, \hat{x}_{v_{bi}}, \hat{p}_{v_{bi}})^\top. \end{aligned} \quad (S2)$$

Next, we consider the column vector of expectation values of the quadratures $\hat{\mathbf{X}}_i$ and the symmetrized covariance matrix Γ_i [1–4] where

$$\bar{\mathbf{X}}_i = (\langle \hat{X}_{i,1} \rangle, \langle \hat{X}_{i,2} \rangle, \langle \hat{X}_{i,3} \rangle, \langle \hat{X}_{i,4} \rangle, \langle \hat{X}_{i,5} \rangle, \langle \hat{X}_{i,6} \rangle, \langle \hat{X}_{i,7} \rangle, \langle \hat{X}_{i,8} \rangle)^\top, \quad (S3)$$

$$\Gamma_i^{kl} = \frac{1}{2} \text{Tr} \left[(\tilde{X}_{i,k} \tilde{X}_{i,l} + \tilde{X}_{i,l} \tilde{X}_{i,k}) \rho \right], \quad (\text{S4})$$

with ρ the density matrix and $\tilde{X}_{i,k} = \hat{X}_{i,k} - \langle \hat{X}_{i,k} \rangle$, $\tilde{X}_{i,l} = \hat{X}_{i,l} - \langle \hat{X}_{i,l} \rangle$. The input-output relation of $\bar{\mathbf{X}}_i$ and Γ_i is described as [5]

$$\bar{\mathbf{X}}_2 = S\bar{\mathbf{X}}_0, \quad (S5)$$

$$\Gamma_2 = S\Gamma_0 S^\top, \quad (S6)$$

where $\bar{\mathbf{X}}_2$ ($\bar{\mathbf{X}}_0$) and Γ_2 (Γ_0) are column vector of expectation values of the quadratures and symmetrized covariance matrix for the output (input) states, respectively, and S is the transformation matrix. In general, the transformation through the first OPA, phase shifter, BSs (loss model) and the second OPA is respectively written as

$$S_{\text{OPA1}} = \begin{pmatrix} \cosh g & 0 & \sinh g & 0 & & \\ 0 & \cosh g & 0 & -\sinh g & 0 & \\ \sinh g & 0 & \cosh g & 0 & & \\ 0 & -\sinh g & 0 & \cosh g & & \\ & & 0 & & & \\ & & & & I & \\ & & & & & \end{pmatrix}_{8 \times 8}, \quad (S7)$$

$$S_\phi^S = \begin{pmatrix} \cos \phi & -\sin \phi & 0 & 0 & & & & \\ \sin \phi & \cos \phi & 0 & 0 & & & & \\ 0 & 0 & 1 & 0 & & & & \\ 0 & 0 & 0 & 1 & & & & \\ & & & & 0 & & & \\ & & & & & \mathbf{I} & & \\ & & & & & & & \\ & & & & & & & \end{pmatrix}_{8 \times 8}, \quad (\text{S8})$$

$$S_\phi^D = \begin{pmatrix} \cos \frac{\phi}{2} & -\sin \frac{\phi}{2} & 0 & 0 & & & & \\ \sin \frac{\phi}{2} & \cos \frac{\phi}{2} & 0 & 0 & & & & \\ 0 & 0 & \cos \frac{\phi}{2} & -\sin \frac{\phi}{2} & & & & \\ 0 & 0 & \sin \frac{\phi}{2} & \cos \frac{\phi}{2} & & & & \\ & & & & 0 & & & \\ & & & & & \mathbf{I} & & \\ & & & & & & & \\ & & & & & & & \end{pmatrix}_{8 \times 8}, \quad (\text{S9})$$

$$S_{\text{loss}} = \begin{pmatrix} \sqrt{T_1} & 0 & 0 & 0 & \sqrt{1-T_1} & 0 & 0 & 0 \\ 0 & \sqrt{T_1} & 0 & 0 & 0 & \sqrt{1-T_1} & 0 & 0 \\ 0 & 0 & \sqrt{T_2} & 0 & 0 & 0 & \sqrt{1-T_2} & 0 \\ 0 & 0 & 0 & \sqrt{T_2} & 0 & 0 & 0 & \sqrt{1-T_2} \\ \sqrt{1-T_1} & 0 & 0 & 0 & -\sqrt{T_1} & 0 & 0 & 0 \\ 0 & \sqrt{1-T_1} & 0 & 0 & 0 & -\sqrt{T_1} & 0 & 0 \\ 0 & 0 & \sqrt{1-T_2} & 0 & 0 & 0 & -\sqrt{T_2} & 0 \\ 0 & 0 & 0 & \sqrt{1-T_2} & 0 & 0 & 0 & -\sqrt{T_2} \end{pmatrix} \quad (\text{S10})$$

$$S_{\text{OPA2}} = \begin{pmatrix} \cosh g & 0 & -\sinh g & 0 & & & & \\ 0 & \cosh g & 0 & \sinh g & & & & \\ -\sinh g & 0 & \cosh g & 0 & & & & \\ 0 & \sinh g & 0 & \cosh g & & & & \\ & & & & 0 & & & \\ & & & & & \mathbf{I} & & \\ & & & & & & & \\ & & & & & & & \end{pmatrix}_{8 \times 8}, \quad (\text{S11})$$

where T_i ($i = 1, 2$) is the transmission parameter of BS describing the losses and we have considered the balanced situation that $\theta_1 = 0$, $\theta_2 = \pi$ and $g_1 = g_2 = g$. S_ϕ^S and S_ϕ^D are the transformation of the phase shifter of single arm case and double arms case, respectively. Therefore, the matrix can be worked out as $S^j = S_{\text{OPA2}} S_{\text{loss}} S_\phi^j S_{\text{OPA1}}$ ($j = S, D$). Next, different output $\bar{\mathbf{X}}_2$ and Γ_2 are given according to the different initial condition $\bar{\mathbf{X}}_0$ and Γ_0 .

A. Coherent and squeezed vacuum state input

With coherent and squeezed vacuum input states ($|\alpha\rangle \otimes |0, \varsigma = re^{i\theta_\varsigma}\rangle$), the initial mean values of quadratures $\bar{\mathbf{X}}_0$ and covariance matrix Γ_0 are given by

$$\bar{\mathbf{X}}_0^{\text{coh\&squ}} = \left(2|\alpha| \ 0 \ 0 \ 0 \ 0 \ 0 \ 0 \ 0 \right)^\top, \quad (\text{S12})$$

$$\Gamma_0^{\text{coh\&sq}} = \begin{pmatrix} 1 & 0 & 0 & 0 & & & & \\ 0 & 1 & 0 & 0 & & & & \\ 0 & 0 & e^{2r} & 0 & & & & \\ 0 & 0 & 0 & e^{-2r} & & & & \\ & & & & 0 & & & \\ & & & & & \mathbf{I} & & \\ & & & & & & & \\ & & & & & & & 8 \times 8 \end{pmatrix}, \quad (\text{S13})$$

where we have let $\theta_\alpha = 0$ and $\theta_\varsigma = \pi$. According to Eqs. (S5) and (S6), we could obtain a mean value vector of 8-dimension ($\bar{\mathbf{X}}_2$) and a covariance matrix of 8×8 -dimension (Γ_2) which describe the output states. Since the modes v_a and v_b represent the bath, we ignore those modes. Then the mean value vector of 4-dimension ($\bar{\mathbf{X}}_2^{\text{ab}}$) and covariance matrix of 4×4 -dimension (Γ_2^{ab}) are extracted from $\bar{\mathbf{X}}_2$ and Γ_2 , respectively. For convenience, we set $T_1 = T_2$ firstly. For phase shift in the single arm case, the $\bar{\mathbf{X}}_2^{\text{ab},S} \equiv (\hat{x}_{a2}, \hat{p}_{a2}, \hat{x}_{b2}, \hat{p}_{b2})$ and $\Gamma_2^{\text{ab},S}$ are given by

$$\bar{\mathbf{X}}_2^{\text{ab},S} = 2\sqrt{T}|\alpha| \begin{pmatrix} (\cosh^2 g \cos \phi - \sinh^2 g) \\ \cosh^2 g \sin \phi \\ \sinh g \cosh g (1 - \cos \phi) \\ \sinh g \cosh g \sin \phi \end{pmatrix}, \quad (\text{S14})$$

$$\Gamma_2^{\text{ab},S} = \begin{pmatrix} \gamma_{11}^S & \gamma_{12}^S & \gamma_{13}^S & \gamma_{14}^S \\ \gamma_{21}^S & \gamma_{22}^S & \gamma_{23}^S & \gamma_{24}^S \\ \gamma_{31}^S & \gamma_{32}^S & \gamma_{33}^S & \gamma_{34}^S \\ \gamma_{41}^S & \gamma_{42}^S & \gamma_{43}^S & \gamma_{44}^S \end{pmatrix}, \quad (\text{S15})$$

where

$$\begin{aligned} \gamma_{11}^S = & e^{-2r} (\cosh^2 g (T \sinh^2 g (e^{4r} \cos^2(\phi) - 2e^{2r} (e^{2r} + 1) \cos(\phi) + \sin^2(\phi) + e^{4r}) - e^{2r} (T - 1)) \\ & + e^{2r} \sinh^2 g (T \sinh^2 g - T + 1) + e^{2r} T \cosh^4 g), \end{aligned} \quad (\text{S16})$$

$$\begin{aligned} \gamma_{12}^S = & (e^{2r} - e^{-2r}) T \sinh^2 g \cosh^2 g \sin(\phi) (\cos(\phi) - 1) \\ = & \gamma_{21}^S, \end{aligned} \quad (\text{S17})$$

$$\begin{aligned} \gamma_{13}^S = & e^{-2r} \sinh g \cosh g (-2e^{2r} (e^{2r} + 1) T \cosh^2 g \sin^2(\frac{\phi}{2}) \\ & + 2(e^{2r} + 1) T \sinh^2 g \sin^2(\frac{\phi}{2}) ((e^{2r} - 1) \cos(\phi) - 1) \\ & + 2e^{2r} (T - 1)) = \gamma_{31}^S, \end{aligned} \quad (\text{S18})$$

$$\begin{aligned} \gamma_{14}^S = & (e^{-2r} + 1) T \sinh g \cosh g \sin(\phi) (\sinh^2 g \\ & \times ((e^{2r} - 1) \cos(\phi) - e^{2r}) + \cosh^2 g) = \gamma_{41}^S, \end{aligned} \quad (\text{S19})$$

$$\begin{aligned} \gamma_{22}^S = & e^{-2r} (\cosh^2 g (T \sinh^2 g (e^{4r} \sin^2(\phi) - 2(e^{2r} + 1) \cos(\phi) + \cos^2(\phi) + 1) \\ & - e^{2r} (T - 1)) + e^{2r} \sinh^2 g (T \sinh^2 g - T + 1) + e^{2r} T \cosh^4 g), \end{aligned} \quad (\text{S20})$$

$$\begin{aligned}\gamma_{23}^S = & (e^{-2r} + 1)T \sinh g \cosh g \sin(\phi)(e^{2r} \cosh^2 g \\ & - \sinh^2 g((e^{2r} - 1) \cos(\phi) + 1)) = \gamma_{32}^S,\end{aligned}\quad (\text{S21})$$

$$\begin{aligned}\gamma_{24}^S = & 2e^{-2r} \sinh g \cosh g (T \sin^2(\phi/2) (\sinh^2 g \\ & (e^{4r}(\cos(\phi) + 1) - \cos(\phi)) + e^{2r} \cosh(2g) \\ & + \cosh^2 g) - e^{2r}(T - 1)) = \gamma_{42}^S,\end{aligned}\quad (\text{S22})$$

$$\begin{aligned}\gamma_{33}^S = & T(e^{-2r} \sinh^4 g \sin^2(\phi) + e^{2r} (\cosh^2 g \\ & - \sinh^2 g \cos(\phi))^2 + \sinh^2(2g) \sin^2(\phi/2) \\ & - \cosh(2g)) + \cosh(2g),\end{aligned}\quad (\text{S23})$$

$$\begin{aligned}\gamma_{34}^S = & 2T \sinh^2 g \sin(\phi) \sinh(2r) (\cosh^2 g \\ & - \sinh^2 g \cos(\phi)) = \gamma_{43}^S,\end{aligned}\quad (\text{S24})$$

and

$$\begin{aligned}\gamma_{44}^S = & T(e^{2r} \sinh^4 g \sin^2(\phi) + e^{-2r} (\cosh^2 g \\ & - \sinh^2 g \cos(\phi))^2 + \sinh^2(2g) \sin^2(\phi/2) \\ & - \cosh(2g)) + \cosh(2g).\end{aligned}\quad (\text{S25})$$

For phase shift in the double arms, $\bar{\mathbf{X}}_2^{\text{ab},\text{D}}$ and $\Gamma_2^{\text{ab},\text{D}}$ are given by

$$\bar{\mathbf{X}}_2^{\text{ab},\text{D}} = \sqrt{2T} |\alpha| \begin{pmatrix} \cos \frac{\phi}{2} \\ \sin \frac{\phi}{2} \cosh(2g) \\ 0 \\ \sin \frac{\phi}{2} \sinh(2g) \end{pmatrix}, \quad (\text{S26})$$

$$\Gamma_2^{\text{ab},\text{D}} = \begin{pmatrix} \gamma_{11}^{\text{D}} & \gamma_{12}^{\text{D}} & \gamma_{13}^{\text{D}} & \gamma_{14}^{\text{D}} \\ \gamma_{21}^{\text{D}} & \gamma_{22}^{\text{D}} & \gamma_{23}^{\text{D}} & \gamma_{24}^{\text{D}} \\ \gamma_{31}^{\text{D}} & \gamma_{32}^{\text{D}} & \gamma_{33}^{\text{D}} & \gamma_{34}^{\text{D}} \\ \gamma_{41}^{\text{D}} & \gamma_{42}^{\text{D}} & \gamma_{43}^{\text{D}} & \gamma_{44}^{\text{D}} \end{pmatrix}, \quad (\text{S27})$$

where

$$\begin{aligned}\gamma_{11}^{\text{D}} = & \frac{1}{4} e^{-2r} [(e^{2r} + 1) T (\cosh 4g - 2 \sinh^2(2g) \cos \phi) \\ & - 4e^{2r}(T - 1) \cosh(2g) + 3e^{2r}T - T],\end{aligned}\quad (\text{S28})$$

$$\gamma_{12}^{\text{D}} = \gamma_{21}^{\text{D}} = 0, \quad (\text{S29})$$

$$\begin{aligned}\gamma_{13}^{\text{D}} = & \frac{1}{4} e^{-2r} [\sinh(4g) T (e^{2r} + 1) (\cos \phi - 1) \\ & + 4e^{2r}(T - 1) \sinh(2g)],\end{aligned}\quad (\text{S30})$$

$$\gamma_{14}^{\text{D}} = e^{-r} T \sinh(2g) \sin(\phi) \cosh(r), \quad (\text{S31})$$

$$\begin{aligned}\gamma_{22}^{\text{D}} = & \frac{1}{4} \{ T [-2 \sinh^2(2g) (e^{2r}(\cos \phi - 1) + \cos \phi) \\ & + \cosh(4g) + 3] - 4(T - 1) \cosh(2g) \},\end{aligned}\quad (\text{S32})$$

$$\gamma_{23}^D = (e^{2r} + 1) T \sinh(g) \cosh(g) \sin(\phi), \quad (\text{S33})$$

$$\begin{aligned} \gamma_{24}^D = & -\frac{1}{4} [(e^{2r} + 1) T \sinh(4g)(\cos(\phi) - 1) \\ & + 4(T - 1) \sinh(2g)], \end{aligned} \quad (\text{S34})$$

$$\begin{aligned} \gamma_{31}^D = & \frac{1}{4} e^{-2r} [(e^{2r} + 1) T \sinh(4g)(\cos(\phi) - 1) \\ & + 4e^{2r}(T - 1) \sinh(2g)], \end{aligned} \quad (\text{S35})$$

$$\gamma_{32}^D = (e^{2r} + 1) T \sinh(g) \cosh(g) \sin(\phi), \quad (\text{S36})$$

$$\begin{aligned} \gamma_{33}^D = & \frac{1}{8} e^{-2r} [-2e^{2r}(T(\cosh(4g) - 1)(\cos(\phi) - 1) \\ & + 4(T - 1) \cosh(2g)) - 2T(\cosh(4g) + 1) \\ & \times (\cos(\phi) - 1) + 4e^{4r}T(\cos(\phi) + 1)], \end{aligned} \quad (\text{S37})$$

$$\gamma_{34}^D = T \cosh(2g) \sin(\phi) \sinh(2r), \quad (\text{S38})$$

$$\gamma_{41}^D = e^{-r} T \sinh(2g) \sin(\phi) \cosh(r), \quad (\text{S39})$$

$$\begin{aligned} \gamma_{42}^D = & -\frac{1}{4} [(e^{2r} + 1) T \sinh(4g)(\cos \phi - 1) \\ & + 4(T - 1) \sinh(2g)], \end{aligned} \quad (\text{S40})$$

$$\gamma_{43}^D = T \cosh(2g) \sin(\phi) \sinh(2r), \quad (\text{S41})$$

and

$$\begin{aligned} \gamma_{44}^D = & \frac{1}{8} e^{-2r} [-2e^{2r}(T(\cosh(4g) - 1)(\cos(\phi) - 1) \\ & + 4(T - 1) \cosh(2g)) - 2e^{4r}T(\cosh(4g) + 1) \\ & \times (\cos(\phi) - 1) + 4T(\cos(\phi) + 1)]. \end{aligned} \quad (\text{S42})$$

So far, the output quadrature vector $\bar{\mathbf{X}}_2^{\text{ab}, j}$ and its covariance matrix $\Gamma_2^{\text{ab}, j}$ ($j = \text{S, D}$) are worked out. Next, we will transform the picture from quadrature operators to creation (annihilation) operators where the corresponding creation and annihilation operator vector $\mathbf{d} = (d_1, d_2, d_3, d_4)^\top \equiv (\hat{a}_2, \hat{a}_2^\dagger, \hat{b}_2, \hat{b}_2^\dagger)^\top$ and its covariance matrix Σ where matrix elements $\Sigma^{u,v} = (1/2)\text{Tr}[\rho(\tilde{d}_u \tilde{d}_v + \tilde{d}_v \tilde{d}_u)]$ with $\tilde{d}_u = d_u - \bar{d}_u$ in terms of $\bar{d}_u = \text{Tr}[\rho d_u]$. The commutation relations are given by $[d_u, d_v] = \Omega^{u,v}$, where

$$\Omega = \begin{pmatrix} 0 & 1 & 0 & 0 \\ -1 & 0 & 0 & 0 \\ 0 & 0 & 0 & 1 \\ 0 & 0 & -1 & 0 \end{pmatrix}. \quad (\text{S43})$$

Equivalently, the relations between $\bar{\mathbf{d}}$ (Σ) and $\bar{\mathbf{X}}_2$ (Γ_2^{ab}) are described as

$$\bar{\mathbf{d}} = H \bar{\mathbf{X}}_2^{\text{ab}}, \quad (\text{S44})$$

$$\Sigma = H \Gamma_2^{\text{ab}} H^\top, \quad (\text{S45})$$

where $\bar{\mathbf{d}} = (\bar{d}_1, \bar{d}_2, \bar{d}_3, \bar{d}_4)^\top$ is mean value of \mathbf{d} and the transformation matrix

$$H = \frac{1}{2} \begin{pmatrix} 1 & i & 0 & 0 \\ 1 & -i & 0 & 0 \\ 0 & 0 & 1 & i \\ 0 & 0 & 1 & -i \end{pmatrix}. \quad (\text{S46})$$

According to Ref. [1], the quantum Fisher information is given by

$$\begin{aligned} \mathcal{F}^{\text{loss}} = & \frac{1}{2} \text{Tr} \{ \partial_\phi \Sigma [\Sigma (\partial_\phi \Sigma)^{-1} \Sigma^\top + \frac{1}{4} \Omega (\partial_\phi \Sigma)^{-1} \Omega^\top]^{-1} \} \\ & + (\partial_\phi \bar{\mathbf{d}})^\top (\Sigma)^{-1} (\partial_\phi \bar{\mathbf{d}}), \end{aligned} \quad (\text{S47})$$

where $\partial_\phi \Sigma = \partial \Sigma / \partial \phi$ and $\partial_\phi \bar{\mathbf{d}} = \partial \bar{\mathbf{d}} / \partial \phi$. Then for two coherent state and squeezed vacuum state input, then the QFIs with loss for phase shift in the single arm is worked out as

$$\mathcal{F}_{\text{coh\&squ}}^{\text{loss, S}} = \frac{N_{\text{coh\&squ}}^{\text{loss, S}}}{D_{\text{coh\&squ}}^{\text{loss, S}}}, \quad (\text{S48})$$

where

$$\begin{aligned} N_{\text{coh\&squ}}^{\text{loss, S}} = & -4e^{5r} \{ 4(T-1)^2 \cosh(8g) \cosh^3(r) (2\alpha^2 + \cosh(2r) + 1) - e^r T^2 \cosh(6g) [16\alpha^2 + (16\alpha^2 + 13) \cosh(2r) \\ & - 4 \cosh(4r) + \sinh(2r) + 10 \sinh(4r) + 6] \} T^3 + 2[-6(T-2)T^2 - 9T + e^{2r} (-8(T-1)\alpha^2 + 26T^2 - 20T + 8) \\ & + 2e^{10r} (T(7T-6) + 2) + e^{8r} (8(5(T-1)T + 2)\alpha^2 + T(32T-29) + 11) + 2e^{4r} [4(T(5T-7) + 4)\alpha^2 + T(10T-9) \\ & + 5] + 4e^{6r} (2(T(10T-11) + 5)\alpha^2 + 6(T-1)T + 3) + 3] \cosh(6g) T^2 + 4(1 + e^{2r}) \{ e^{6r} [4\alpha^2(T(3T-2) + 5)(T-1)^2 \\ & + T^2 (4T^2 - 2T - 1) + 1] + T(T(T(13T-22) + 15) - 4) + e^{8r} (T-1)(T(T(13T-19) + 13) - 3) \\ & + e^{4r} (8((T-2)T + 3)((T-1)T + 1)\alpha^2 + T(T(2(19 - 9T)T - 27) + 8) + 1) \\ & + e^{2r} (-4(T-1)(T((T-1)T + 3) + 1)\alpha^2 + T(T(2T(2T-7) + 21) - 12) + 3) \} \cosh(4g) T \\ & + 8e^{5r} \cosh^2(r) ((T(T((186 - 95T)T - 173) + 80) - 18) \cosh(r) + (T(T(T(75T-146) + 129) - 56) + 10) \cosh(3r) \\ & + 2(2T-1)(T(37T-34) + 19) \sinh(r) + 2(T((31 - 22T)T - 20) + 5) \sinh(3r)) T \\ & + 4\alpha^2 e^{2r} [-e^{6r} (T(T(13T-8) + 4) - 16)(T-1)^2 + T(T(3(T-1)T - 4) - 12)(T-1) + e^{2r} (T(T(T(22 - 7T) \\ & + 13) + 16) - 12) + 16] + e^{4r} (T(T(T((62 - 23T)T - 147) + 120) - 60) + 32) \\ & - 2 \cosh(2g) \{ 8e^{2r} [T(3T^2 + T - 4) - e^{6r} (T-1)(T^2(T(2T-3) + 6) - 4) \\ & + e^{4r} (T(T(-4T^3 + 10T^2 + T - 3) + 4) - 8) - e^{2r} (T(T(T(T(2T-5) + 19) - 8) + 4) + 4) \} \alpha^2 \\ & + 4e^{5r} T \cosh^2(r) ((-(T-1)T(2T(66T-65) + 101) - 16) \cosh(r) + ((T-1)T(2T(58T-57) + 89) + 16) \cosh(3r) \\ & - 2(2T-1)(-33(T-1)T + (31(T-1)T + 16) \cosh(2r) - 16) \sinh(r) \}, \end{aligned} \quad (\text{S49})$$

and

$$\begin{aligned} D_{\text{coh\&squ}}^{\text{loss, S}} = & -16[(e^{2r} + 1)(T^2 - T) \cosh(2g) - e^{2r} \\ & \times (T-1)^2 - T^2] \{ (e^{2r} + 1)^2 (T-1)T [(T-1)T \\ & \times \cosh(4g) - 4((T-1)T + 1) \cosh(2g)] + e^{4r} \\ & \times (T-1)^2 (3T^2 + 2) + 2e^{2r} [2 + T(3T((T-2)T \\ & + 3) - 4)] + (T-1)^2 (3T^2 + 2) \}, \end{aligned} \quad (\text{S50})$$

and for phase shift in the double arms is worked out as

$$\begin{aligned} \mathcal{F}_{\text{coh\&squ}}^{\text{loss, D}} = & \frac{T [1 + e^{2r} \tanh^2(2g)] + e^{2r} (1 - T) / \cosh(2g)}{(1 - T) [e^{2r} (2 \sinh^2 g - 1/T) + \cosh(2g)] + T} \\ & \times N_\alpha \cosh^2(2g) - \frac{C^D}{D^D}, \end{aligned} \quad (\text{S51})$$

where

$$\begin{aligned} C^D &= e^{-2r} (e^{2r} + 1)^2 T^2 [T(e^{2r} + 1)^2 (T - 1) \cosh(6g) \\ &\quad - 4(e^{4r} + 1) (T^2 - T + 1) \cosh(4g) \\ &\quad - (18e^{2r} - 7e^{4r} - 7) (T - 1) T \cosh(2g) \\ &\quad - 4(e^{4r} - 4e^{2r} + 1) (T^2 - T + 1)], \end{aligned} \quad (\text{S52})$$

$$\begin{aligned} D^D &= 8[(e^{2r} + 1)^2 (T - 1)^2 T^2 \cosh(4g) \\ &\quad - 4(e^{2r} + 1)^2 (T^3 - 2T^2 + 2T - 1) T \cosh(2g) \\ &\quad + (22e^{2r} + 3e^{4r} + 3) T^2 + 8e^{2r} (1 - 2T) \\ &\quad + (e^{2r} + 1)^2 (3T^4 - 6T^3)]. \end{aligned} \quad (\text{S53})$$

B. Two coherent states input

With coherent and squeezed vacuum input states ($|\alpha_0\rangle \otimes |\beta\rangle$), the initial mean values of quadratures $\bar{\mathbf{X}}_0$ and covariance matrix Γ_0 are given by

$$\begin{aligned} \bar{\mathbf{X}}_0^{\text{coh\&coh}} &= (2|\alpha| \ 0 \ 2|\beta| \cos \theta_\beta \ 2|\beta| \sin \theta_\beta \\ &\quad 0 \ 0 \ 0 \ 0)^\top, \end{aligned} \quad (\text{S54})$$

$$\Gamma_0^{\text{coh\&coh}} = I_{8 \times 8}, \quad (\text{S55})$$

where for convenience we let $\theta_\alpha = 0$. In a similar way as the above, for phase shift in the single arm case, the $\bar{\mathbf{X}}_2^{\text{ab,S}}$ and $\Gamma_2^{\text{ab,S}}$ are given by

$$\bar{\mathbf{X}}_2^{\text{ab,S}} = \sqrt{2T} \begin{pmatrix} M_1^S \\ M_2^S \\ M_3^S \\ M_4^S \end{pmatrix}, \quad (\text{S56})$$

where

$$\begin{aligned} M_1^S &= |\alpha|(\cosh^2 g \cos \phi - \sinh^2 g) - |\beta| \sinh(2g) \sin(\phi/2) \\ &\quad \times \sin(\phi/2 - \theta_\beta), \\ M_2^S &= \cosh(g)[|\alpha| \cosh g \sin \phi + |\beta| \sinh g (\sin(\phi - \theta_\beta) \\ &\quad + \sin \theta_\beta)], \\ M_3^S &= [|\alpha| \sinh(2g) \sin^2(\phi/2) - |\beta|(\sinh^2 g \cos(\phi - \theta_\beta) \\ &\quad - \cosh^2 g \cos \theta_\beta)], \\ M_4^S &= [|\alpha| \sinh g \cosh g \sin \phi + |\beta|(\sinh^2 g \sin(\phi - \theta_\beta) \\ &\quad + \cosh^2(g) \sin \theta_\beta)], \end{aligned} \quad (\text{S57})$$

and

$$\Gamma_2^{\text{ab,S}} = \begin{pmatrix} \gamma_{11}^S & \gamma_{12}^S & \gamma_{13}^S & \gamma_{14}^S \\ \gamma_{21}^S & \gamma_{22}^S & \gamma_{23}^S & \gamma_{24}^S \\ \gamma_{31}^S & \gamma_{32}^S & \gamma_{33}^S & \gamma_{34}^S \\ \gamma_{41}^S & \gamma_{42}^S & \gamma_{43}^S & \gamma_{44}^S \end{pmatrix}, \quad (\text{S58})$$

where

$$\begin{aligned}
\gamma_{11}^S &= \cosh(2g)(T \cosh 2g - T + 1) - T \sinh^2(2g) \cos \phi \\
&= \gamma_{22}^S = \gamma_{33}^S = \gamma_{44}^S, \\
\gamma_{12}^S &= \gamma_{21}^S = \gamma_{34}^S = \gamma_{43}^S = 0 \\
\gamma_{13}^S &= \sinh(2g)[T \cosh 2g(\cos \phi - 1) + T - 1] \\
&= \gamma_{31}^S, \\
\gamma_{14}^S &= T \sinh(2g) \sin \phi \\
&= \gamma_{41}^S = \gamma_{23}^S = \gamma_{32}^S, \\
\gamma_{24}^S &= \sinh(2g)(T \cosh 2g - T + 1) - \frac{1}{2}T \sinh(4g) \cos \phi, \\
&= \gamma_{42}^S,
\end{aligned} \tag{S59}$$

For phase shift in the double arms, $\bar{\mathbf{X}}_2^{\text{ab},\text{D}}$ and $\Gamma_2^{\text{ab},\text{D}}$ are given by

$$\bar{\mathbf{X}}_2^{\text{ab},\text{D}} = \sqrt{2T} \begin{pmatrix} M_1^D \\ M_2^D \\ M_3^D \\ M_4^D \end{pmatrix}, \tag{S60}$$

where

$$\begin{aligned}
M_1^D &= |\alpha_0| \cos(\phi/2) + |\beta_0| \sinh(2g) \sin(\phi/2) \sin \theta_\beta, \\
M_2^D &= \sin(\phi/2)(|\alpha_0| \cosh(2g) + |\beta_0| \sinh(2g) \cos \theta_\beta), \\
M_3^D &= |\beta_0| (\cos(\phi/2) \cos \theta_\beta - \cosh(2g) \sin(\phi/2) \sin \theta_\beta), \\
M_4^D &= \sin(\phi/2)|\alpha_0| \sinh(2g) + |\beta_0|[\sin(\phi/2) \cos \theta_\beta \cosh(2g) \\
&\quad + \cos(\phi/2) \sin \theta_\beta]
\end{aligned} \tag{S61}$$

and

$$\Gamma_2^{\text{ab},\text{D}} = \begin{pmatrix} \gamma_{11}^D & \gamma_{12}^D & \gamma_{13}^D & \gamma_{14}^D \\ \gamma_{21}^D & \gamma_{22}^D & \gamma_{23}^D & \gamma_{24}^D \\ \gamma_{31}^D & \gamma_{32}^D & \gamma_{33}^D & \gamma_{34}^D \\ \gamma_{41}^D & \gamma_{42}^D & \gamma_{43}^D & \gamma_{44}^D \end{pmatrix}, \tag{S62}$$

$$\begin{aligned}
\gamma_{11}^D &= \cosh(2g)(T \cosh(2g) - T + 1) - T \sinh^2(2g) \cos(\phi) \\
&= \gamma_{22}^D = \gamma_{33}^D = \gamma_{44}^D, \\
\gamma_{12}^D &= \gamma_{34}^D = 0, \\
\gamma_{13}^D &= \sinh(2g)[T \cosh(2g)(\cos \phi - 1) + T - 1], \\
&= \gamma_{31}^D, \\
\gamma_{14}^D &= T \sinh(2g) \sin \phi \\
&= \gamma_{41}^D, \\
\gamma_{23}^D &= T \sinh(2g) \sin \phi \\
&= \gamma_{32}^D, \\
\gamma_{24}^D &= \sinh(2g)[T \cosh(2g) - T + 1] - \frac{1}{2}T \sinh(4g) \cos \phi \\
&= \gamma_{42}^D.
\end{aligned} \tag{S63}$$

Therefore, for two coherent states ($|\alpha\rangle \otimes |\beta\rangle$) input, the QFIs with loss for phase shift in the single arm is worked out as

$$\begin{aligned} \mathcal{F}_{\text{coh\&coh}}^{\text{loss, S}} = & \frac{T^2 \sinh^2(2g)}{2(1-T)T \sinh^2(g) + 1} \\ & + \frac{4T(T \cosh 2g + 1 - T)}{4(1-T)T \sinh^2(g) + 1} \times [N_{\text{in}}^{\text{coh\&coh}} \cosh^2 g \\ & + \sqrt{N_\alpha N_\beta} \sinh(2g) \cos(\theta_\beta) - N_\beta], \end{aligned} \quad (\text{S64})$$

and for phase shift in the double arms is worked out as

$$\mathcal{F}_{\text{coh\&coh}}^{\text{loss, D}} = \frac{N_{\text{coh\&coh}}^{\text{loss, D}}}{D_{\text{coh\&coh}}^{\text{loss, D}}}, \quad (\text{S65})$$

where

$$\begin{aligned}
N_{\text{coh\&coh}}^{\text{loss, D}} = & -T(T-1) \cosh(2g) [N_{\text{in}}^{\text{coh\&coh}} (3T^2 - 2T + 2) \\
& - T^2] + T^2 \cosh(4g) [N_{\text{in}}^{\text{coh\&coh}} (3T^2 - 4T + 3) + 2T \\
& \times (T-1) + 1] - T^3 (T-1) \cosh(6g) (N_{\text{in}}^{\text{coh\&coh}} + 1) \\
& + T^2 [N_{\text{in}}^{\text{coh\&coh}} (T-1)^2 - 2T(T-1) - 1] + 4\sqrt{N_{\alpha} N_{\beta}} \\
& \times T \sinh(2g) \cos(\theta_{\beta}) [T(3T^2 - 4T + 3) \cosh(2g) \\
& - (T-1)(T^2 \cosh 4g + 2T^2 - T + 1)], \tag{S66}
\end{aligned}$$

$$D_{\text{coh\&coh}}^{\text{loss, D}} = 2[2(1-T)T \sinh^2(g) + 1] \times [4(1-T)T \sinh^2(g) + 1]. \quad (\text{S67})$$

In the body of the article, we use the losses rate $L = 1 - T$ to describe the QFI and QCRB.

- [1] Y. Gao and H. Lee, Bounds on quantum multiple-parameter estimation with Gaussian state, *Eur. Phys. J. D* **68**, 347 (2014).
- [2] A. Monras, Phase space formalism for quantum estimation of Gaussian states, *arXiv:1303.3682v1* (2013).
- [3] S. L. Braunstein, and P. van Loock, Quantum information with continuous variables, *Rev. Mod. Phys.* **77**, 513 (2005).
- [4] C. Weedbrook, S. Pirandola, R. García-Patrón, N. J. Cerf, T. C. Ralph, J. H. Shapiro, and S. Lloyd, Gaussian quantum information, *Rev. Mod. Phys.* **84**, 621 (2012).
- [5] G. Adesso, S. Ragy, and A. R. Lee, Continuous Variable Quantum Information: Gaussian States and Beyond, *Open Systems & Information Dynamics* **21**, 1440001 (2014).